Colloids and Surfaces B: Biointerfaces 114 (2014) 269–276

Contents lists available at ScienceDirect

Colloids and Surfaces B: Biointerfaces

journal homepage: www.elsevier.com/locate/colsurfb

Effect of particle size on conformation and enzymatic activity of EcoRI adsorbed on CdS nanoparticles

Yonghai Song[a], Dandan Zhong[a], Dan Luo[a], Mei Huang[a], Zhenzhong Huang[a], Hongliang Tan[a], Lanlan Sun[b], Li Wang[a,*]

[a] Key Laboratory of Functional Small Organic Molecule, Ministry of Education, College of Chemistry and Chemical Engineering, Jiangxi Normal University, Nanchang 330022, People's Republic of China

[b] State Key Laboratory of Luminescence and Applications, Changchun Institute of Optics, Fine Mechanics and Physics, Chinese Academy of Sciences, 3888 East Nan-Hu Road, Changchun 130033, People's Republic of China

ARTICLE INFO

Article history:
Received 13 July 2013
Received in revised form 4 October 2013
Accepted 14 October 2013
Available online 22 October 2013

Keywords:
CdS nanoparticles
EcoRI
Cooperativity
Conformation change
Enzymatic activity

ABSTRACT

Better understanding of the interaction between nanoparticles (NPs) and protein is the basis for biological and biomedical applications of NPs. Water-soluble fluorescent CdS NPs have been widely used in the biological and biomedical fields and the study on effect of CdS NPs size on conformation and enzymatic activity of protein might be very important in its application. In this work, the interaction of CdS NPs with different size with type II restriction endonuclease (EcoRI) were investigated by atomic force microscopy, transmission electron microscopy, UV–vis spectroscopy, fluorescence quenching method, CD spectra, laser scanning confocal microscopy and gel electrophoresis. It was found that the equilibrium constant (k_D) as well as the cooperativity degree of CdS NPs-EcoRI binding (Hill constant, n) strongly depended on the CdS NPs size. The different curvature of CdS NPs surface could result in different changes of EcoRI conformation. The gel electrophoresis indicated that the decrease in α-helix content more or less affected the activity of EcoRI.

© 2013 Elsevier B.V. All rights reserved.

1. Introduction

The rapid development of nanotechnology in the past decades offers wide prospects for micro- and nano-scale materials in various areas, such as industry, biotechnology, and biomedicine, etc. There has been particular interest in using nanoparticles (NPs) to probe biological process which is critical for diagnostics, the modulation of cell functions and sensors [1–3]. From the biological and biomedical application of viewpoint, the primary interest stems from the fact that NPs are small enough to interact with cellular machinery and to reach previously inaccessible targets, such as the brain [4,5]. Therefore, there are numerous studies on the interaction between NPs and biomolecules for designing the safe nano-biomaterials.

On the basis of the motivation described above, we settled on an initial focus on the interaction between CdS NPs and type II restriction endonuclease (EcoRI) [6]. EcoRI is chose as a typical representative because EcoRI is an important biomacromolecule in lives cells and is considered to be part of defense system that protects bacterial cells against foreign DNA [6]. The conjugation of proteins to nanoscale colloidal particles has been well studied since the development of immunoprobes in the early 1970s [7]. Moreover, a large number of studies on proteins or peptide adsorbed on Au NPs with different sizes have been performed. In the interaction process, these proteins undergo a partial loss or change of structure and generally a significant loss in enzyme activity [8–11]. This may affect the protein functions, which is crucial for biological systems. Thus, it should be expected that particle size plays a key role in modulating protein structure and function. However, no systematic study has been performed to date on the effect of nanoscale particle size on the structure and function of adsorbed proteins, independent of NPs surface chemistry.

For this reason, we carried out a systematic study on EcoRI adsorbed to difference-sized CdS NPs ranging from 1.17 ± 0.64 to 21.62 ± 5.31 nm, which have similar surface chemistry, since CdS NPs have been widely used in the biological and biomedical fields. The mechanism of EcoRI–CdS NPs interaction, the binding (or association) constant of the EcoRI with CdS NPs, changes of EcoRI conformation upon adsorption on the different curvature of the CdS NPs surface were explored in detail. Specifically, fluorescence quenching measurements gave information about the EcoRI–CdS NPs binding kinetics, equilibrium and change of EocRI conformation. Circular dichroism (CD) spectrum revealed the changes in EcoRI secondary structure upon binding. And the gel

* Corresponding author. Tel.: +86 791 88120861; fax: +86 791 88120861.
E-mail addresses: lwanggroup@yahoo.com.cn, lwangsy2003@hotmail.com (L. Wang).

0927-7765/$ – see front matter © 2013 Elsevier B.V. All rights reserved.
http://dx.doi.org/10.1016/j.colsurfb.2013.10.020

electrophoresis monitored enzyme activity after it was conjugated with CdS NPs. The results might be of interest to physical chemists and material scientists.

2. Material and methods

2.1. Materials

Sodium sulfide ($Na_2S{\cdot}9H_2O$) and anhydrous cadmium chloride ($CdCl_2$) were obtained from Aladdin (Shanghai, China) and 11-mercaptoundecanoic acid (MUA, 95%) was purchased from Sigma-Aldrich (St. Louis, USA). EcoRI (from *Escherichia coli* RY13) was obtained from Takara (Dalian, China). Sodium phosphate (AR) and other reagents were bought from Beijing Chemical Reagent Factory (Beijing, China) and were of analytical reagent grade. The phosphate buffer solution (PBS, 0.2 M) were prepared by mixing solution of 0.2 M Na_2HPO_4 and 0.2 M NaH_2PO_4. All solutions were prepared with ultrapure water purified by a Millipore-Q System (18.2 MΩ cm). Muscovite mica ($KA1_2(AlSi_3)O_{10}(OH)_2$, V-1 grade) was purchased from Linhe Street Commodity Marketplace (Changchun, China) and was cut into 1 cm × 1 cm square pieces as AFM substrates.

2.2. Preparation of CdS NPs

CdS NPs with different sizes (1.17 ± 0.64 to 21.62 ± 5.31 nm) were synthesized according to our previous method [6]. Briefly, appropriate amounts of $CdCl_2$ and $Na_2S{\cdot}9H_2O$ were dissolved in ultrapure water separately. MUA was dropped into the $CdCl_2$ solution slowly with continuous stirring at 30 °C under N_2, and the pH was adjusted to 10.0 using 0.1 M NaOH solution. Subsequently, Na_2S solution was dropped quickly into the mixture solution with constant stirring, and a clear yellowish suspension of CdS NPs was obtained. The initial molar ratio of Cd/MUA/S was approximately 1:5:1. Then the mixture was transferred into a Teflon lined stainless steel autoclave of 25 mL capacity and heated at 75 °C for 6 h. To obtain CdS NPs with different sizes, the molar ratios of MUA to Cd were changed to 4:1, 2:1 and 1:1 with a constant molar ratio of Cd/S of 1:1, respectively. The products were washed three times with anhydrous ethanol and ultrapure water alternately. The aqueous CdS NPs suspension was stored in a refrigerator at 4 °C. The CdS NPs have similar surface chemistry (hydrophilic COOH-terminated surface), which ensures that any difference in interaction with protein is primarily due to the effect of NPs size.

2.3. Preparation of the EcoRI–CdS NPs bioconjugates

The EcoRI–CdS NPs bioconjugates were prepared as followed. The EcoRI and CdS NPs were mixed in 500 μL 0.2 M PBS and then the mixture was incubated at 4 °C for at least 1 h. A series of the bioconjugates with different CdS NPs concentration were prepared by keeping the concentration of EcoRI constant (0.03 U μL^{-1}). To maintain their original conformational states in the solution, and prevent shear forces from disrupting the structure of the bioconjugates, no separation techniques (i.e., centrifugation or filtration) were used in the experiment.

2.4. UV–vis absorption and fluorescence spectra measurements

The UV–vis absorption spectra were measured with a Perkin–Elmer Lambda 35 spectrophotometer. All experiments were performed with a conventional quartz cell of 1 cm path length. The fluorescence spectra were obtained using a Perkin–Elmer LS 55 luminescence spectrometer. The emission spectra of each system were measured with a fixed excitation wavelength of 280 nm and the fluorescence of EcoRI was measured to investigate effect of CdS NPs size on the conformation and enzymatic activity of EcoRI adsorbed on CdS NPs. The EcoRI concentration was 0.03 U μL^{-1} and CdS NPs concentration is varied in the experiment. Appropriate blanks corresponding to the PBS were subtracted to correct the fluorescence background. The experiments were repeated for seven times and found to be reproducible within experimental errors.

2.5. Atomic force microscopy (AFM) measurements

AFM measurements were carried out with an AJ-III AFM system (Shanghai Aijian Nanotechnology) in tapping mode. Standard silicon (Si) cantilevers (spring constant, 0.6–6 N m^{-1}) were used under its resonance frequency (typically, 60–150 kHz). All AFM images were acquired at room temperature under ambient conditions. A 10 μL aqueous solution containing CdS NPs (1.67 mM) was dropped onto a freshly cleaved mica surface and kept for 15 min. After that, the mica sample was rinsed with ultrapure water and dried in air for AFM imaging of CdS NPs.

2.6. Transmission electron microscopy (TEM) measurements

A FEI, Technai-S-twin electron microscope operating at an acceleration voltage of 200 kV was used for TEM imaging. Samples were prepared by dropping the CdS NPs suspension on the surface of carbon-coated copper grid and drying them in air.

2.7. Laser scanning confocal microscopy

The images were collected using a Leica TCS SP2 microscope (from Leica Microsystems Heidelberg GmbH), with excitation at 380 nm. Liquid dot films for observation (0.13–0.17 mm final thickness) were prepared by spreading a few drops of the suspensions on the surface of an optical dish mounted on the microscope stage. The excitation beam was vertically propagated and images representing luminescence emission of defined-thickness horizontal cross-sections were collected over a scanning time of 0.1–0.5 s per image. Each image corresponded to a scan over an area of 18.0 μm × 12.0 μm and 0.13 mm thick cross-section, with the exact image size determined by microscope objective and focusing parameters. Emission spectra were collected from 400 to 720 nm. Signal collection time was optimized for best contrast.

2.8. Circular dichroism (CD) spectroscopy

The far-UV CD spectra of EcoRI adsorbed on CdS QDs were recorded on a Jasco model J-820 CD spectropolarimeter (Jasco, Tokyo, Japan) at 25 °C using cylindrical quartz cuvettes with a 1 cm path length. The measurements were performed in 5 mM PBS (pH 6.0) for native EcoRI (1.3 U μL^{-1}) and EcoRI–CdS NPs bioconjugate. The CD spectra were recorded over the range 190–240 nm at a scan rate of 200 nm min^{-1}. The final spectrum was the average of three scans after correction for the unspecific dichroic absorbance of the medium by computer manipulation.

2.9. Gel electrophoresis

The gel electrophoresis experiments were performed on Mini-PROTEAN Tetra Cell (Bio-Rad Laboratories Instruments Co., USA). The agarose gel was prepared in TAE buffer at 1.0% final agarose concentration for enzyme activity assays. Appropriately sized wells (15 μL) were formed by placing a comb in the center of the gel. A 10 μL λ-DNA stock solution containing 100 ng DNA and a 10 μL mixed solution containing 100 ng λ-DNA, 4 U EcoRI (or EcoRI–CdS NPs) and 1 μL 10 × *H* buffer were prepared. The solutions were incubated at 37 °C in thermostat water bath for 1 h. Then the solutions were added into wells of gels, respectively. A constant voltage

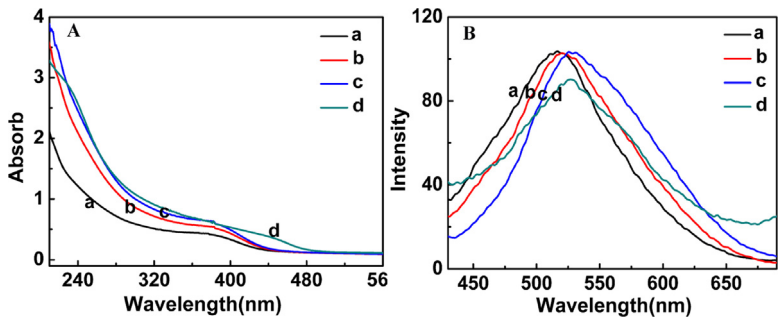

Fig. 1. UV–vis absorption (A) and fluorescence spectra (B) of CdS NPs prepared with the Cd^{2+}/S^{2-} = 1:1 and [MUA]/[Cd^{2+}] molar ratio of 5:1 (a), 4:1 (b), 2:1 (c), 1:1 (d), respectively.

(120 V) was applied for 25 min for sufficient separation. Finally, the gel was stained in gelred staining solution.

3. Results and discussions

3.1. Characterization of CdS NPs

Fig. 1A presented the UV–vis absorption spectrum of the MUA-capped CdS NPs with different size. These samples showed well-defined first excitonic absorption peaks at 362 nm (curve *a*), 384 nm (curve *b*), 400 nm (curve *c*), and 440 nm (curve *d*), respectively. They were typical characteristic of the plasmon resonance adsorption of CdS NPs [12,13]. The shift in the absorption peak position corresponded to the increase in the diameter of the CdS NPs [14]. In Fig. 1B, it could be seen that the fluorescence peak position varied from 513 to 530 nm in a similar way with the change of CdS NPs diameter (curve *a*–*d*). The difference between the emission peak position and the absorption edge indicated that the present CdS NPs exhibited trap-state emission rather than

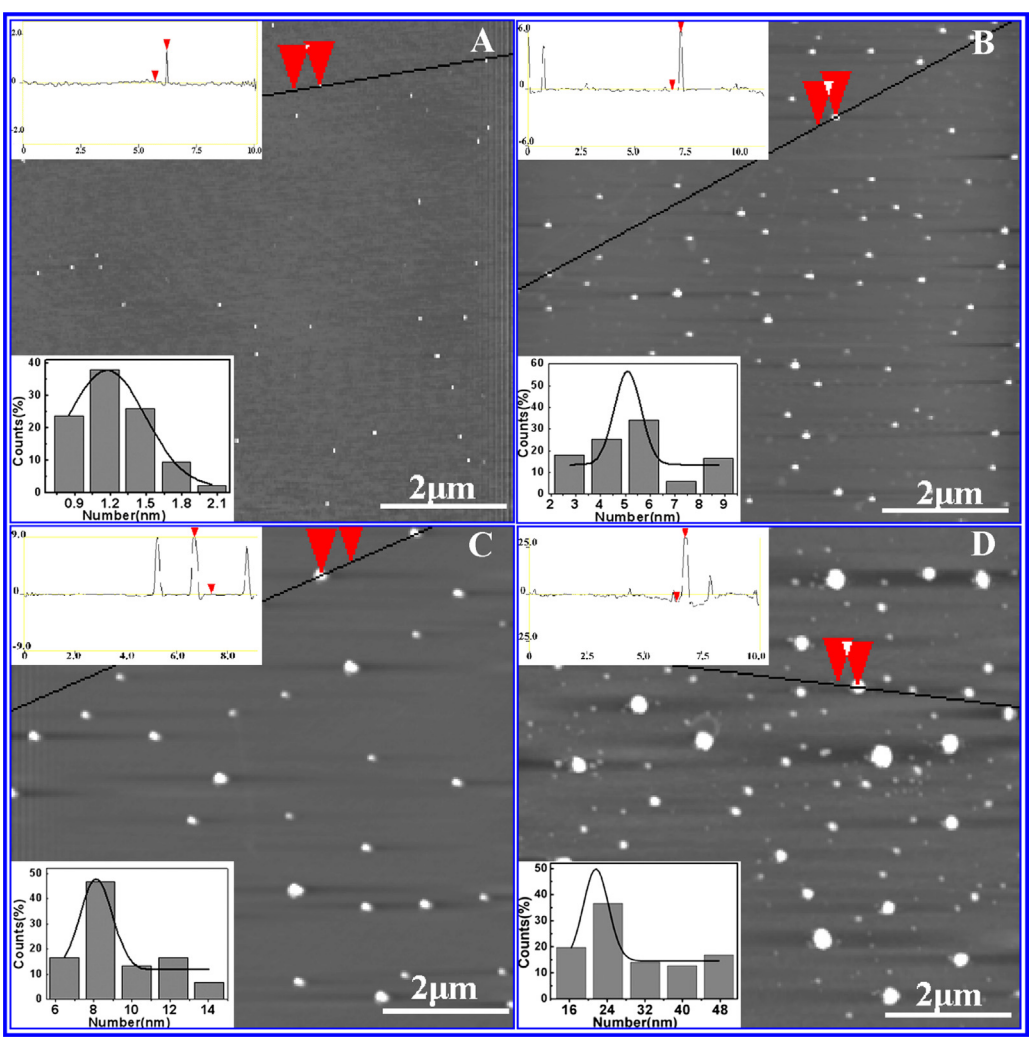

Fig. 2. AFM images of CdS NPs with different sizes: (A) 1.17 ± 0.64 nm, (B) 5.10 ± 1.06 nm, (C) 8.13 ± 1.69 nm and (D) 21.62 ± 5.31 nm. The insets showed the size distribution and section analysis for each sample.

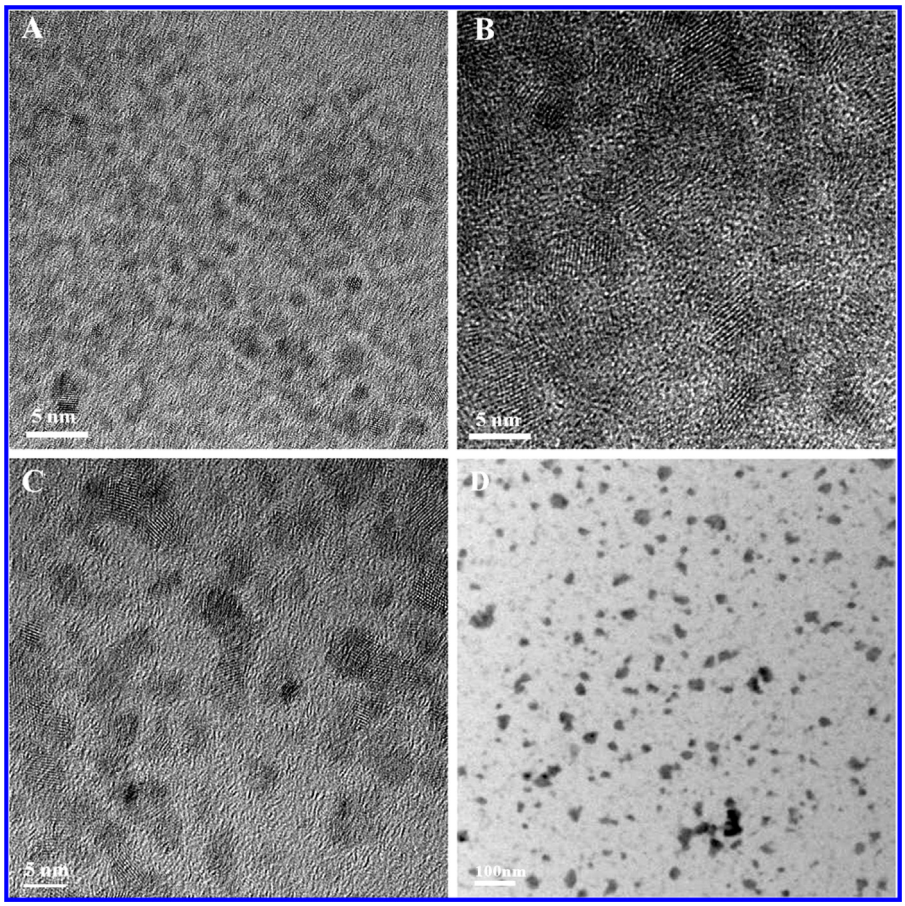

Fig. 3. TEM images of CdS NPs with different sizes: (A) 1.17 ± 0.64 nm, (B) 5.10 ± 1.06 nm, (C) 8.13 ± 1.69 nm and (D) 21.62 ± 5.31 nm.

band-edge emission. The observed broad fluorescence peak was commonly attributed to the recombination of charged carriers trapped in the surface states, which was related to the size of CdS NPs [15–19]. Thus, the quantum effect happened, directing the emission peaks to blue-shift.

AFM was used to measure the size of the MUA-capped CdS NPs. Fig. 2 showed the AFM images of the MUA-capped CdS NPs with different size deposited onto mica surface. The images clearly showed the nearly spherical shape of particles dispersed on mica surface uniformly. Section analysis could be used to determine the size of particles. The insets in Fig. 2 showed the statistical histogram of the size of the CdS NPs which was about 1.17 ± 0.64 nm (Fig. 2A), 5.10 ± 1.06 nm (Fig. 2B), 8.13 ± 1.69 nm (Fig. 2C), and 21.62 ± 5.31 nm (Fig. 2D), respectively. It should be noted that the size of the particles were measured according to the height but not width because the AFM tip radius would affect the measurement. Typical TEM images of the specimens were shown in Fig. 3: 1.17 ± 0.64 nm (Fig. 3A), 5.10 ± 1.06 nm (Fig. 3B), 8.13 ± 1.69 nm (Fig. 3C) and 21.62 ± 5.31 nm (Fig. 3D). According to a statistical analysis of the TEM results, the diameters of well-dispersed individual CdS NPs were consistent with those in AFM measurements. It also revealed that CdS NPs were mostly spherical and single crystals.

3.2. Interaction mechanism between EcoRI and CdS NPs

The laser scanning confocal microscopy was used to image CdS NPs and CdS NPs-EcoRI conjugates. Images of CdS NPs and the same CdS NPs conjugated with EcoRI by electrostatic attraction were shown in Fig. 4A and B, respectively. The images represented the luminescence emission along the excitation path from thin cross-sections which were directly adjacent to the support surface. Each bright point represented emission from an individual CdS NPs center within the cross-sections in sample A and B. The images are essentially identical to the features of those observed in previous single dot spectroscopy [20,21]. These dots on the unconjugated CdS NPs image were homogeneously dispersed, and the amounts of the dots in the image were less as compared with the image of CdS NPs–EcoRI. Images taken from CdS NPs conjugated with EcoRI also showed that luminescent centers homogeneously distributed over each cross-section, similar to the dispersion of unconjugated CdS NPs. However, a substantially higher density of luminescent centers was observed for EcoRI–CdS NPs, due to the larger quantum yield of the conjugated CdS NPs [20] The conjugation of CdS NPs with EcoRI offered a large number of functional groups, such as thiol, $-NH_2$, –OH, –COOH, which could be helpful for passivating the electronic defects on the surface of the CdS NPs and accordingly the luminescence was enhanced [22].

3.3. Fluorescence quenching of EcoRI by CdS NPs with different sizes

The application of fluorescence spectroscopy to study on the structure and conformation of proteins has been proven to be fruitful [23–28]. The emission characteristics of tryptophan, tyrosine, and phenylalanine residues in protein can provide a convenient handle for investigating the binding and conformation changes upon association with NPs. The interaction between CdS NPs and EcoRI was also investigated by fluorescence quenching of EcoRI by CdS NPs. In this study, the EcoRI concentration was kept at about

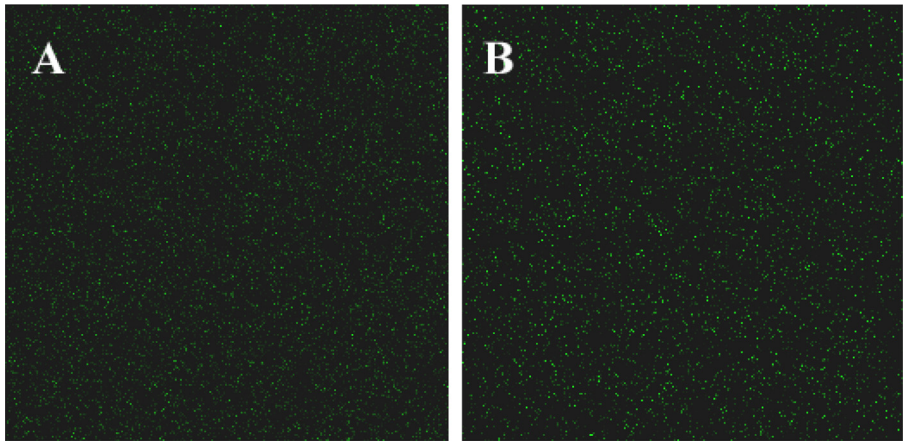

Fig. 4. Laser scanning fluorescence images of cross-sectional slices along the *z* direction for 1.17 ± 0.64 nm CdS NPs aqueous samples: (A) unconjugated CdS NPs and (B) CdS NPs–EcoRI bioconjugates.

0.03 U μL^{-1} and the CdS NPs concentration was varied in the four samples. Once the EcoRI associated with the CdS NPs, tyrosine and tryptophan residues was accessible to the surface of the CdS NPs then their fluorescence was quenched as shown in Fig. 5. Thus, the change of fluorescence emission spectrum intensity (I_{max}) resulted from the change of EcoRI conformation [29–33]. In the present case, it was due to the adsorption of EcoRI onto the CdS NPs, which reflected relative changes in the proximity between the active fluorescence emitters (tyrosine or tryptophan) in the EcoRI and the quenching agent of CdS NPs. As shown in Fig. 5, the process was accompanied by the appearance of an isosbestic point, indicating the presence of intermediates during conjugation. The presence of the isosbestic point also suggested the change of the excited state energy [34].

To better understand the EcoRI–CdS NPs binding interaction and explore how CdS NP size affected the binding property, the binding cooperativity was investigated by using Hill equation. The Hill coefficient (n) was frequently utilized to measure the binding cooperativity [35]. The upper insets of Fig. 5 showed Hill plots associated with the EcoRI–CdS NPs binding measurements. The fluorescence quenching could be quantified by the following equation [36,37]:

$$Q = \frac{(I_0 - I)}{I_0} \quad (1)$$

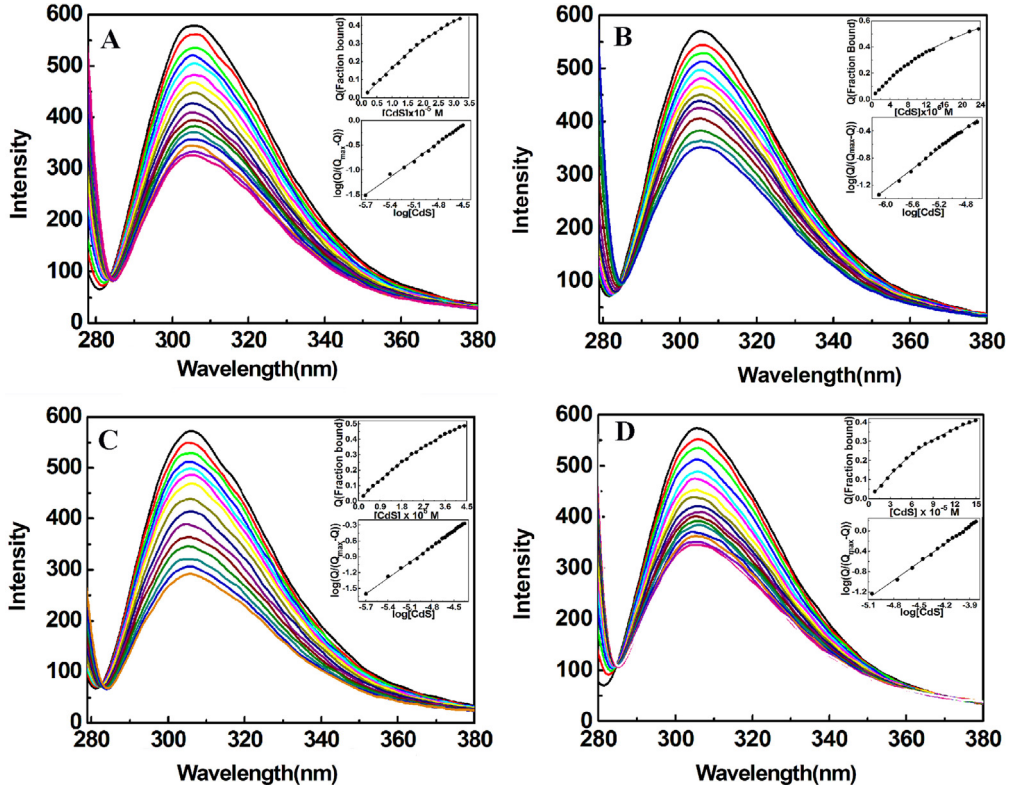

Fig. 5. Fluorescence quenching of EcoRI by different CdS NPs: (A) 1.17 ± 0.64 nm, (B) 5.10 ± 1.06 nm, (C) 8.13 ± 1.69 nm and (D) 21.62 ± 5.31 nm. The concentration of EcoRI was 0.03 U μL^{-1}. The upper insets corresponded to the binding curves of the EcoRI to CdS NPs, and lower insets showed the transformation of binding curves by the Hill equation 2. Data were fitted to equation 3 (solid line) with different CdS NPs sizes.

Table 1
CdS NPs–EcoRI binding parameters obtained from fluorescence quenching data.

	CdS_A	CdS_B	CdS_C	CdS_D
Q_{max}	0.99 ± 0.12	1.27 ± 0.094	1.4 ± 0.16	0.68 ± 0.04
n	1.16 ± 0.02	1.23 ± 0.056	0.998 ± 0.01	1.18 ± 0.01
k_D	7.24×10^{-6}	6.02×10^{-7}	8.32×10^{-5}	2.09×10^{-5}
R^2	0.997	0.963	0.999	0.998
RSD (n = 7, %)	1.73	4.37	1.15	2.22

A, B, C and D indicated the size of CdS NPs were 1.17 ± 0.64 nm, 5.10 ± 1.06 nm, 8.13 ± 1.69 nm and 21.62 ± 5.31 nm, respectively.

where I_0 and I were fluorescence intensities in the absence and presence of CdS NPs, respectively, Q was the binding density, Q_{max} was the saturation value of Q. It was assumed that the binding of EcoRI to CdS NPs occurred at equilibrium, and accordingly the Q and the CdS NPs concentration could be fitted by Hill equation (also called Langmuir equation). Based on the upper insets in Fig. 5, the Q_{max} could be obtained and the data were summarized in Table 1. It could be seen that the small particles had a low Q_{max}, indicating the binding of EcoRI onto the small CdS NPs was less than that of the big CdS NPs. Then the fluorescence quenching data for Q would be further fitted to determine an equilibrium constant (k_D) which described the EcoRI–CdS NPs interaction. Since a given protein could be expected to have multiple associative interactions with NPs, the binding equilibrium might exhibit cooperativity as the classic example of binding of multiple O_2 molecules to hemoglobin [37]. Conventionally, the complex phenomenon was taken into account by modeling Q through the Hill equation [36,37]:

$$\frac{Q}{Q_{max}} = \frac{[NP]^n}{(k_D + [NP]^n)} = \frac{[NP]^n}{(k_a^n + [NP]^n)} \quad (2)$$

$$\log \left(\frac{Q}{(Q_{max} - Q)}\right) = n\log \ [NP] - \log \ k_D \quad (3)$$

where k_D was the EcoRI–CdS NPs equilibrium constant, and n was the Hill coefficient. Although the modeling based on Eq. (3) was somewhat idealized, n was generally regarded as a measure of associated "cooperativity". A positive cooperative reaction ($n > 1$) suggested that once one protein molecule was bound to the NPs, its affinity for the NPs progressively increased in a superlinear fashion. For a negative cooperative reaction ($n < 1$), the binding strength of the protein to NPs became progressively weaker as further adsorption of proteins. For a noncooperative association, where $n = 1$ and Q formally has the mathematical form of Langmuir adsorption equation [36,37], the affinity of the proteins for NPs was independent on whether other protein molecules were already bound. The binding constant K was defined to be the reciprocal of k_D.

The cooperativities of the binding processes were further diagnosed by the slope n of the Hill plot of $\log(Q/(Q_{max} - Q))$ versus log[CdS], which were shown in the lower insets of Fig. 5 [38,39]. The value of n increased with the degree of cooperativity and the possible maximum value of n was equal to the number of possible binding sites. In the Hill plot, the fitting to the date allowed us to determine the k_D and n and they were listed in Table 1. It was found that all the values of n were approximatively larger than 1, indicating the binding of EcoRI to the surface of CdS NPs had a positive cooperativity.

In Table 1, the equilibrium constant k_D for EcoRI–CdS NPs increased progressively as CdS NPs diameter increased. A similar trend has been established in the chemisorptions of oligonucleotide chains to CdS NPs. A less efficient polymer surface packing was observed in larger NPs, because of the enhancement of the excluded volume interactions within the extended random coil nucleotide chains on the particle surface [40]. So, proteins (or EcoRI) in unfolded conformations should exhibit a similar behavior. This comparison emphasized the potential role of the conformational state of the adsorbed proteins in understanding the nature of protein layers that formed on NPs and the variation of k_D with NPs size. Geometrical accommodation of EcoRI bound onto the NPs surface was discriminatory. Measurements on individual of k_D for individual protein-NPs systems had given a rough idea of the relative rates in this competitive multi-component adsorption process when particle and protein concentration effects on rates were considered.

3.4. Conformation of EcoRI in EcoRI–CdS NPs bioconjugates

It was known that some proteins bound to the NPs surface and retained their native-like structure, while others undergone denaturation of their tertiary structure, and even their secondary structure could be disrupted in some cases [31,41]. Moreover, the protein might be bound in a preferred orientation [42]. The degree of denaturation depended on NPs surface chemistry, as well as its NPs surface curvature. CD spectroscopy was used to explore in detail how the adsorption of EcoRI on CdS NPs influenced the protein conformation. Here, the CdS NPs with 1.17 ± 0.64, 5.10 ± 1.06, 8.13 ± 1.69 and 21.62 ± 5.31 nm in diameter were used.

The far-UV region (190–250 nm) of the CD spectrum in a solution, corresponding to peptide bond absorption, was employed to study the secondary structure of EcoRI. It was known that when a polypeptide chain existed in the α-helical conformation, there were two negative minima at 208 and 222 nm, and a positive band at 190 nm [43]. The band at 208 nm corresponded to π–π* transition of the α-helix, whereas the band at 222 nm corresponded to π–π* transition for both the α-helix and random coil [44]. For the existence of a β-sheet, a positive and a negative band appeared at 190 and 215 nm, respectively. The intensities of bands at both 208 and 222 nm were found to decrease in the bioconjugates system (Fig. 6A) as compared to that of the native EcoRI, indicating the α-helix content decreased as the size of the NPs increased. The α-helix content decreased from about 35.4% for free EcoRI to about 29.7% for EcoRI adsorbed on 21.62 ± 5.31 nm CdS NPs, and the relative amount of different conformations were showed by the inset of Fig. 6A. It was clear that the amount of α-helix decreased, β-sheet and random coil increased.

The mechanism behind the effect of the surface curvature on protein structure could be explained by a simple model. A flat surface provided a larger area to contact the adsorbed proteins, which resulted in stronger interaction between proteins and NPs and greater perturbation of the protein structure. However, there were several exceptions, such as RNase A, whose degree of denaturation increased with increasing of surface curvature [45], and chymotrypsinogen, who lost the secondary structure and enzymatic activity on both curved and flat surfaces [46–48]. The results obtained for EcoRI was that, when it was adsorbed on a large surface curvature (small NPs), the α-helices was almost retained, and gradual decreasing in the surface curvature (NPs less than 20 nm) resulted in the increasing of the β-sheet structure. The conformation change after the protein adsorbed on NPs might also depend on the flexibility or tertiary structure of protein. When the protein with a high flexibility or weak tertiary structure absorbed on the NPs surface, the large surface curvature (small NPs) would result in a large change of conformation due to good match to surface curvature. When the protein with a poor flexibility or strong tertiary structure absorbed on the NPs surface, its tertiary structure was only slightly disturbed. As a consequence, the small surface curvature (big NPs) would result in a large change of conformation due to strong interaction between protein and big NPs. Therefore, our result might also be ascribed to the poor flexibility or strong tertiary structure of EcoRI, which resulted in large change of conformation on small surface curvature.

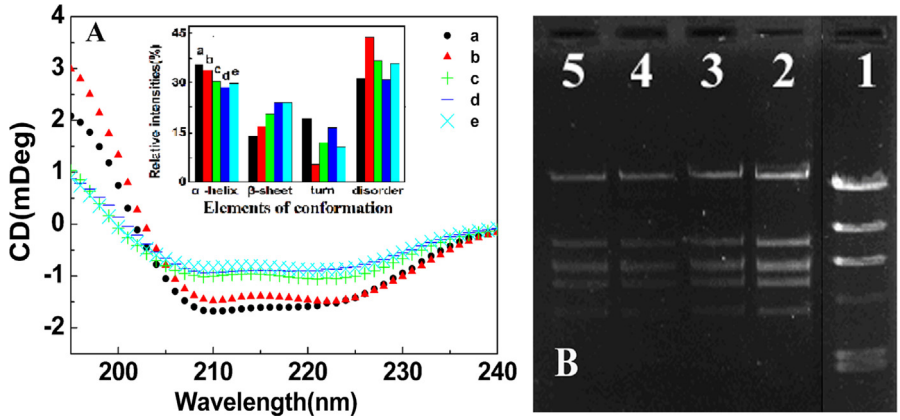

Fig. 6. (A) Far UV–CD spectra of EcoRI (1.3 U μ.L^{-1}) or EcoRI–CdS NPs bioconjugates. Inset: Relative amounts of different conformations in (a) pure EcoRI and EcoRI–CdS NPs with different CdS sizes: (b) 1.17± 0.64 nm, (c) 5.10 ± 1.06 nm, (d) 8.13 ± 1.69 nm and (e) 21.62 ± 5.31 nm. (B) agarose gels analysis of λ-Hind III digest DNA marker (lane 1), λ-DNA digested with EcoRI/CdS$_A$ NPs (lane 2), λ-DNA digested with EcoRI/CdS$_B$ NPs (lane 3), λ-DNA digested with EcoRI/CdS$_C$ NPs (lane 4) and λ-DNA digested with EcoRI/CdS$_D$ NPs (lane 5).

3.5. Enzyme activity assays

Fig. 6B showed the bands of λ-DNA marker and λ-DNA digested by EcoRI or EcoRI–CdS NPs bioconjugates on the agarose gel after electrophoresis. EcoRI is an endonuclease enzyme isolated from strains of *E. coli*, and is part of the restriction modification system. In molecular biology, it creates sticky ends with 5′ end overhangs. The nucleic acid sequence where the enzyme cuts is GAATTC, which, as the complementary sequence is CTTAAG, has rotational symmetry [49]. It could be clearly seen that EcoRI cut the λ-DNA (lane 2, 3, 4, 5) as compared to the lane of marker (lane 1), which indicated that the EcoRI bound on CdS NPs with different size also existed bioactivity. The lane became lighter gradually with the increase of NPs size, indicating that EcoRI activity was slightly influenced by the size of CdS NPs.

4. Conclusions

A systematic measurement to quantify the interaction between CdS NPs with different size and EcoRI was performed. The relative cooperativity of the protein bound onto CdS NPs was dependent on the CdS NPs size, and the k_D increased with the increase of CdS NPs size. Furthermore, the conformation of EcoRI bound onto CdS NPs was changed and the change degree of the conformation increased as the CdS NPs size increased. And more native-like enzyme activity for EcoRI adsorbed on smaller CdS NPs was retained. The results reported herein provided the evidence that smaller NPs, perhaps because of their greater surface curvature, promoted the retention of more native-like protein structure and function as compared to that on larger particle. Hence, this study contributed to a better understanding of the size effect to CdS NPs–EcoRI interactions, which was a reference for applications of CdS NPs in vivo.

Acknowledgments

This work was financially supported by National Natural Science Foundation of China (20905032, 21065005, 21165010 and 21101146), Young Scientist Foundation of Jiangxi Province (20112BCB23006 and 20122BCB23011), Foundation of Jiangxi Educational Committee (GJJ13243 and GJJ13244), the State Key Laboratory of Electroanalytical Chemistry (SKLEAC201310), the Open Project Program of Key Laboratory of Functional Small Organic Molecule, Ministry of Education, Jiangxi Normal University (no. KLFS-KF-201214; KLFS-KF-201218).

References

[1] J.M. Nam, C.S. Thaxton, C.A. Mirkin, Science 301 (2003) 1884.
[2] W.J. Liu, Z.N. Zhu, K. Deng, Z.T. Li, Y.L. Zhou, H.B. Qiu, Y. Gao, S.N. Che, Z.Y. Tang, J. Am. Chem. Soc. 135 (2013) 9659.
[3] Z.T. Li, Z.N. Zhu, W.J. Liu, Y.L. Zhou, B. Han, Y. Gao, Z.Y. Tang, J. Am. Chem. Soc. 134 (2012) 3322.
[4] M. Mahmoudi, M.A. Sahraian, M.A. Shokrgozar, S. Laurent, ACS Chem. Neurosci. 2 (2011) 118.
[5] M. Nic Ragnaill, M. Brown, D. Ye, M. Bramini, S. Callanan, I. Lynch, K.A. Dawson, Eur. J. Pharm. Biopharm. 77 (2011) 360.
[6] Y.H. Song, D. Luo, S.H. Ye, M. Huang, D.D. Zhong, Z.Z. Huang, H.Q. Hou, L. Wang, Phys. Chem. Chem. Phys. 14 (2012) 16258.
[7] W.P. Faulk, G.M. Taylor, Immunocytochemistry 8 (1971) 1081.
[8] S. Lindman, I. Lynch, E. Thulin, H. Nilsson, K.A. Dawson, S. Linse, Nano Lett. 7 (2007) 914.
[9] S.H. De Paoli Lacerda, J.J. Park, C. Meuse, D. Pristinski, M.L. Becker, A. Karim, J.F. Douglas, ACS Nano 4 (2010) 365.
[10] T.L. Jennings, M.P. Singh, G.F. Strouse, J. Am. Chem. Soc. 128 (2006) 5462.
[11] C. Czeslik, R. Winter, Phys. Chem. Chem. Phys. 3 (2001) 235.
[12] Z.H. Zhang, W.S. Chin, J.J. Vittal, J. Phys. Chem. B 108 (2004) 18569.
[13] Y.L. Zhou, Z.N. Zhu, W.X. Xiao, W.J. Liu, S.J. Wu, X.F. Liu, Y. Gao, W. Zhang, Z.Y. Tang, Angew. Chem. Int. Ed. 50 (2011) 11456.
[14] P. Mandal, S.S. Talwar, S.S. Major, R.S. Srinivasa, J. Chem. Phys. 128 (2008) 114703.
[15] C.H. Fischer, A. Henglein, J. Phys. Chem. 93 (1989) 5578.
[16] H. Fujiwara, H. Hosakawa, K. Murakoshi, Y. Wada, S. Yanazida, T. Okada, H. Kobayashi, J. Phys. Chem. B 101 (1997) 8270.
[17] D. Diaz, M. Rivera, T. Ni, J.C. Rodriguez, S.E. Castillo-Blum, D. Nagesha, J. Robles, O.J. Alvarez-Fregoso, N.A. Kotov, J. Phys. Chem. B 103 (1999) 9854.
[18] G. Carrot, S.M. Scholz, C.J.G. Plummer, J.G. Hilborn, J.L. Hedrick, Chem. Mater. 11 (1999) 3571.
[19] Y.L. Zhou, M. Yang, K. Sun, Z.Y. Tang, N.A. Kotov, J. Am. Chem. Soc. 132 (2010) 6006.
[20] M. Nirmal, B.O. Dabbousi, M.G. Bawendi, J.J. Macklin, J.K. Trautman, T.D. Harris, L.E. Brus, Nature 383 (1996) 802.
[21] S.A. Empedocles, R. Neuhauser, M.G. Bawendi, Nature 399 (1999) 126.
[22] D. Ghosh, S. Mondal, S. Ghosh, A. Saha, J. Mater. Chem. 22 (2012) 699.
[23] X.C. Shen, X.Y. Liou, L.P. Ye, H. Liang, Z.Y. Wang, J. Colloid Interface Sci. 311 (2007) 400.
[24] D.J. Gao, Y. Tian, S.Y. Bi, Y.H. Chen, A.M. Yu, H.Q. Zhang, Spectrochim. Acta, Part A 62 (2005) 1203.
[25] C. Wang, Q.H. Wu, C.R. Li, Z. Wang, J.J. Ma, X.H. Zang, N.X. Qin, Anal. Sci. 23 (2007) 429.
[26] V. Anbazhagan, R.S. Damai, A. Paul, M. Swamy, Biochim. Biophys. Acta 1784 (2008) 891.
[27] M. Noronha, J.C. Lima, E. Paci, H. Santos, A.L. Macanita, Biophys. J. 92 (2000) 4401.
[28] S. Gorinstein, I. Goshev, S. Moncheva, M. Zemser, M. Weisz, A. Caspi, I. Libman, H.T. Lerner, S. Trakhtenberg, O. Martin-Belloso, J. Protein Chem. 19 (2000) 637.
[29] S.H. Brewer, W.R. Glomm, M.C. Johnson, M.K. Knag, S. Franzen, Langmuir 21 (2005) 9303.
[30] N. Chadborn, J. Bryant, A.J. Bain, P. O'Shea, Biophys. J. 76 (1999) 2198.
[31] P. Roach, D. Farrar, C.C. Perry, J. Am. Chem. Soc. 127 (2005) 8168.
[32] F.L. Cui, J.L. Wang, Y.R. Cui, J.P. Li, Anal. Chim. Acta 571 (2006) 175.
[33] Q. Xiao, S. Huang, Z.D. Qi, B. Zhou, Z.K. He, Y. Liu, Biochim. Biophys. Acta 1784 (2008) 1020.
[34] L.J. Libertini, E.W. Small, Biophys. J. 47 (1985) 765.
[35] A.V. Hill, Biochem. J. 7 (1913) 471.

[36] P.K. Jain, W.Y. Huang, M.A. El-Sayed, Nano Lett. 7 (2007) 2080.
[37] E.M. De La Cruz, J. Mol. Biol. 346 (2005) 557.
[38] L. Stryer, Biochemistry, Freeman & Company, New York, NY, 1995.
[39] M. Lei, P. Baumann, T.R. Cech, Biochemistry 41 (2002) 14560.
[40] H.L. Huang, Y.G. Xu, H.Y. Low, Polymer 46 (2005) 5949.
[41] S.K. Ghosh, A. Pal, S. Kundu, S. Nath, T. Pal, Chem. Phys. Lett. 395 (2004) 366.
[42] Y.H. Ding, Z.Q. Chen, J. Xie, R. Guo, J. Colloid Interface Sci. 327 (2008) 243.
[43] N. Vigneshwaran, A.A. Kathe, P.V. Varadarajan, R.P. Nachane, R.H. Balasubramanya, Langmuir 23 (2007) 7113.
[44] V.M. Bolanos-Garcia, S. Ramos, R. Castillo, J. Xicohtencatl-Cortes, J. Mas-Oliva, J. Phys. Chem. B 105 (2001) 5757.
[45] W. Shang, J.H. Nuffer, J.S. Dordick, R.W. Siegel, Nano Lett. 7 (2007) 1991.
[46] J.E. Gagner, M.D. Lopez, J.S. Dordick, R.W. Siegel, Biomaterials 32 (2011) 7241.
[47] A. Garland, L. Shen, X.Y. Zhu, Prog. Surf. Sci. 87 (2012) 1.
[48] J.E. Gagner, X. Qian, M.M. Lopez, J.S. Dordick, R.W. Siegel, Biomaterials 33 (2012) 8503.
[49] M.R. Kurpiewski, L.E. Engler, L.A. Wozniak, A. Kobylanska, M. Koziolkiewicz, W.J. Stec, L. Jen-Jacobson, Structure 12 (2004) 1775.